Remote Sensing of Lake Chicot, Arkansas: Monitoring Suspended Sediments, Turbidity, and Secchi Depth with Landsat MSS Data

John A. Harrington, Jr. and Frank R. Schiebe
Water Quality and Watershed Research Laboratory, USDA/ARS, Durant, Oklahoma

Joe F. Nix
Ouachita Baptist University, Arkadelphia, Arkansas

This research used water quality data from Lake Chicot, Arkansas and a corresponding set of Landsat MSS data to compare the ability of satellite-based sensor systems to monitor suspended sediment concentration, Secchi disk depth, and nephelometric turbidity. Lake Chicot was selected, in part, because of the availability of a wide range of water quality conditions. Secchi disk depth and nephelometric turbidity are both optical measures of water quality and differ from suspended sediment concentration, which is a measure of the weight of inorganic particulates suspended in the water column. Four different models for these relationships between the satellite data and the water quality data were tested: 1) simple linear regression analysis with the satellite data transformed to exoatmospheric reflectance, 2) a simple linear regression involving a natural logarithm transformation of the satellite and water quality variables, 3) simple linear regression analysis of the digital chromaticity transformation of the satellite data and the natural logarithm of the water quality data, and 4) optimized curve fitting of a theoretically derived exponential model for the relationship between exoatmospheric reflectance and the water quality data. Two different solar spectral irradiance curves and an orbital eccentricity correction factor are tested using the exponential model. Results suggest: 1) Remote sensing from space-based platforms can provide meaningful information on water quality variability; 2) an exponential model best characterizes the relationship between the satellite data and the water quality measures investigated; 3) slight differences result from using the solar curve proposed by the World Radiation Center (as opposed to the NASA standard); and 4) predictions based on optical measures of water quality, rather than measures of the weight of particles in the water column, are slightly better when using Landsat MSS data.

Address correspondence to Frank R. Schiebe, Water Quality and Watershed Research Lab., USDA/ARS, Durant, OK 74702.
Received 17 May 1990; revised 16 June 1991.

INTRODUCTION

A number of methods exist for *in situ* observations of inorganic contaminants in surface waters (USGS, 1979). Observations of Secchi disk depth, nephelometric turbidity, and suspended sediment concentration (among other measures) provide quantitative information concerning water quality conditions and can be used in various numerical

ISSN/92/$0.00
Published 1992 by Elsevier Science Publishing Company, Inc.

schemes to help characterize the trophic state of an aquatic ecosystem (e.g., Carlson, 1977). *In situ* measurements of water quality characteristics tend to be limited, especially in the temporal and spatial domains, because of the costs associated with data collection and laboratory analyses. Satellite remote sensing provides an alternative means for obtaining relatively low-cost, simultaneous information on surface water conditions from numerous lakes situated within a large geographic area (Carpenter and Carpenter, 1983; Lathrop and Lillesand, 1986; Lillesand et al., 1983; Lindell et al., 1986; Lyon et al., 1988; Ritchie et al., 1987; Ritchie and Cooper, 1988; Shih and Gervin, 1980; Verdin, 1985). With over 18 years of Landsat multispectral scanner (MSS) sensor data now available, temporal changes in water quality can also be monitored (Harrington et al., 1989).

This article addresses the ability to use Landsat MSS data to estimate surface water quality using data from Lake Chicot, Arkansas. Two distinct basins with differiing water quality characteristics occur within this oxbow lake, and a considerable amount of water quality field data has been collected. In addition, the water of Lake Chicot has been the subject of several previous remote sensing investigations concerned with monitoring suspended sediments as an indication of lake water quality.

In situ studies at Lake Chicot used a handheld spectroradiometer to examine incident and reflected solar radiation for wavelengths between 400 nm and 1500 nm (Ritchie et al., 1983). Lake Chicot sediments were resuspended in a 11,600-L tank at the Marine Upwelled Spectral Signature Laboratory (MUSSL) at NASA's Langley Research Center to examine the upwelled radiance for suspended sediment concentrations that ranged up to 700 mg L^{-1} (Witte et al., 1981). Photointerpretation of Landsat MSS images for the period 1972–1979 provided an indication of the origin, geographic pattern, and temporal variation of turbidity in the lake (LeCroy, 1982). Initial examination of Landsat TM data indicated that Bands 1–4 have potential for use in analysis of suspended sediment concentration and that Band 3 demonstrated the greatest promise (Schiebe et al., 1985).

Previous analyses of the utility of Landsat MSS digital data for water quality monitoring have been conducted using Lake Chicot data. The first studies (Ritchie and Schiebe, 1986; Schiebe and Ritchie, 1986) used a data set consisting of 63 observations from 33 dates during the period 1976–1979. Simple linear and multiple regression techniques indicated that MSS Band 3 (700–800 nm) was the best single band for explaining variations in suspended sediment. The Lake Chicot data set of corresponding water quality and Landsat MSS observations has been expanded to 310 observations from 79 dates for the period 1976–1987 and examination of this data set provides substantial evidence to support a theoretical-based exponential relationship between suspended sediments and reflectance (Schiebe et al., 1987).

This article advances beyond these previous studies and uses the Lake Chicot data set of Landsat MSS and corresponding water quality observations to compare the established ability of satellite-based sensor systems to monitor suspended sediment concentration with the ability to monitor for nephelometric turbidity and Secchi disk depth. Nephelometric turbidity and Secchi disk depth are both optical measures of water quality and, therefore, differ from suspended sediment concentration, which is a measure of the weight of inorganic particulates suspended in the water column. Four different models for these relationships between the satellite data and the water quality data were tested. Results suggest that 1) remote sensing from space-based platforms can provide meaningful information on water quality variability and 2) optical measures of water quality (i.e., nephelometric turbidity and Secchi depth), rather than measures of the weight of particles in the water column (i.e., suspended sediment concentration), are slightlly better predicted using Landsat MSS data.

STUDY AREA

Lake Chicot (Fig. 1) was formed approximately 600 years ago by the meandering of the Mississippi River. Located in Chicot County in southeastern Arkansas (between 33°06'N and 33°23'N and 91°10'W and 91°17'W), the oxbow lake has a surface area of 17.2 km^2, a width of 1.0 km, and a shoreline of 58.2 km, and is the largest natural lake in Arkansas. Historically, Lake Chicot was a clean lake with good fishing and a high recreational value, but significant changes have oc-

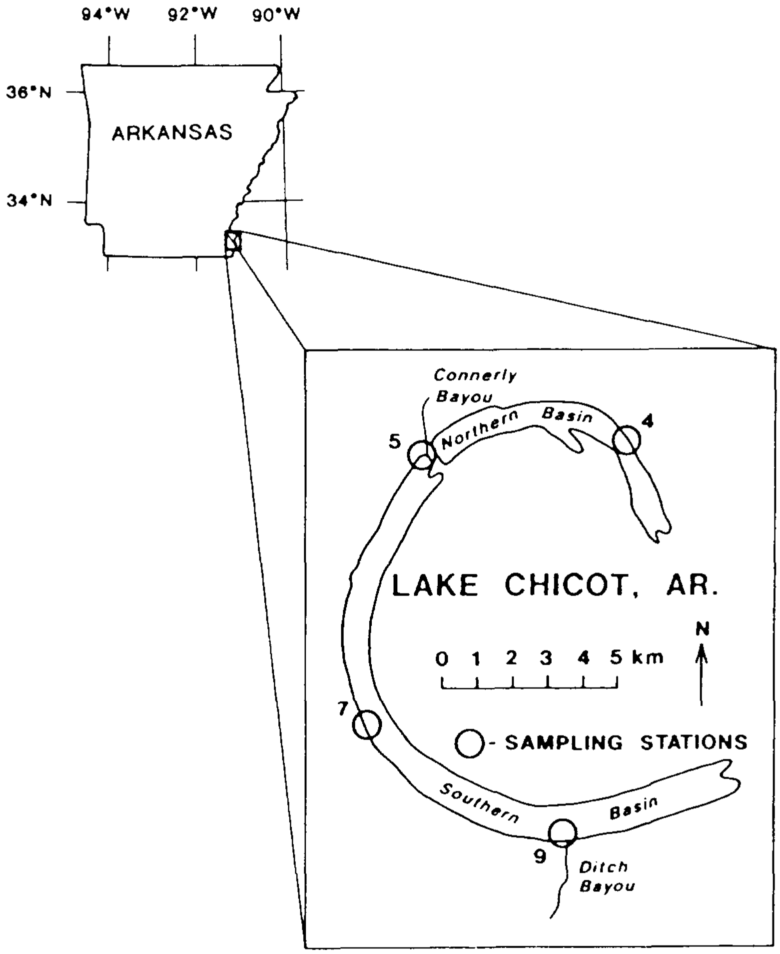

Figure 1. Lake Chicot, Arkansas reference map showing the four sampling site locations.

curred during the 20th century. As a result of a major Mississippi River flood in 1927, the Lake Chicot watershed was enlarged to a catchment area of 930 km^2. The flood scoured the inlet, Connerly Bayou, and built a natural sand spit or levee that partially separated the lake into two separate basins. There were pronounced differences between the two basins, with the northern basin receiving ephemeral runoff from a relatively small 25 km^2 area, while the southern basin was trapping sediments and chemicals associated with runoff from an area of cotton and soybean agriculture. In the 1960s, legislation authorized the development and implementation of plans for lake restoration. A major research effort (Nix and Schiebe, 1984) provided data on lake limnology and developed a physically based, process-oriented model of lake processes (Stefan et al., 1984). The model now provides guidance for the operation of three hydrologic engineering structures (a gravity flow/pump facility and dams at both the inlet and outlet). These structures divert flows laden with large amounts of suspended sediments into the Mississippi River and regulate lake levels. Since initial operation of these structures in April 1985, there has been a significant reduction in suspended sediment levels in the southern basin of Lake Chicot (Harrington et al., 1989).

DATA

Water quality data for Lake Chicot were originally collected every 2 weeks for development and testing of the lake processes model (Nix and Schiebe, 1984). Beginning in October 1981, arrangements were made for the water quality samples to be collected on the day of Landsat flyover (weekend flyovers were sampled on the adjacent week day). Water quality characteristics were determined for four sites within Lake Chicot (Fig. 1) and included pH, Secchi disk depth, total solids, dissolved solids, nephelometric turbidity, chlorophyll a, conductivity, temperature, dissolved oxygen, and a number of measures of nutrient levels. Suspended sediment concentration was calculated as the difference between total solids (measured by weighing the residue obtained from evaporating a 100 mL sample) and dissolved solids (measured by weighing the residue after filtering a 100 mL sample through a 0.45 μm filter and evaporating the filtrate).

Landsat MSS digital numbers or their estimates were obtained from densitometer analysis of negative transparencies (Schiebe et al., forthcoming), computer compatible tapes (CCTs), and 8 in. floppy diskettes that are compatible with the Remote Image Processing System (RIPS) (Welch et al., 1983). From the digital data sources, a 5×5 pixel array for each of the four bands of the Landsat MSS was extracted for each water quality sample site location. A sample of 25 pixels is small enough to avoid contamination by shoreline effects produced in the EDIPS digital data processing (Verdin, 1983), is thought to be large enough to provide reasonable statistics (means and standard deviations), and is large enough to identify potential bias by a miscalibrated scanner (Ritchie and Cooper, 1987).

The Landsat MSS data set was transformed to the physical values of radiance and exoatmospheric reflectance (Robinove, 1982) using procedures outlined in Markham and Barker (1986) and values of solar spectral irradiance determined using linear interpolation from both the NASA standard solar spectral irradiance curve (Thekaekara, 1970) and using the solar curve proposed by the World Radiation Center (Iqbal, 1983). The solar spectral irradiance values for each Landsat MSS band-width were adjusted for changes in Earth–Sun distance using an eccentricity correction factor (Iqbal, 1983). These steps were necessary because the Landsat MSS database for Lake Chicot includes observations from all five Landsat MSS sensor systems and from all months of the year.

Beginning in the fall of 1981, surface water quality data were collected to coincide with the time of satellite flyover. Prior to this time, estimates of water quality characteristics were determined using two methods: 1) linear interpolation of measurements made from before and after the date of satellite overpass, and 2) use of the lake water quality model developed by Stefan et al. (1984). Estimated values provided by the model run were evaluated with knowledge of daily weather events and the value obtained through linear interpolation; in all cases the model output was selected to be used in comparisons with the Landsat MSS data.

METHODS

All of the analyses in this research involved transformation of the raw Landsat MSS digital numbers or their estimates. The digital chromaticity transformation of the satellite data was performed using the procedures detailed in Lindell et al. (1986). Radiance values were corrected to a sun elevation of 90° and used in the calculation of the x, y, and z chromaticity indices. Linear regression analyses were then performed between the x, y, and z chromaticity indices and the natural logarithm transformation of each of the water quality measures as suggested by Munday and Alfoldi (1979).

Previous research demonstrated that exoatmospheric reflectance, calculated by correcting the satellite data for differences in sensor characteristics and sun elevation angle, provided that better explanation of the concentration of suspended sediments (i.e., higher coefficients of determination) when compared with either radiance or raw digital numbers (Schiebe et al., 1987). Thus, it was decided that Landsat MSS data transformed to exoatmospheric reflectance would be used in all the remaining analyses of this study. Two methods were used to examine the relationship between the selected water quality parameters (suspended sediment concentration, Secchi disk depth, and nephelometric turbidity) and the satellite data. First, simple linear regression techniques were used to analyze the relationship between the water quality parameters and exoatmospheric reflectance, primarily because this technique has been widely used in previous studies (Lyon et al., 1988; Munday and Alfoldi, 1979; Ritchie et al., 1986; Ritchie et al., 1987; Shih and Gervin, 1980). In addition, simple linear regression was also performed following a natural logarithm transform of both variables.

Finally, an optimized, curve-fitting technique (DeCoursey and Snyder, 1969) based on the use of an exponential relationship between suspended sediment concentration and exoatmospheric reflectance was also tested. Theoretical considerations involving Beer's law were used in deriving an exponential relationship between exoatmospheric reflectance (Ri) and suspended sediment concentration (SSc), which has the form

$$\mathrm{Ri} = \mathrm{Ai} + (\mathrm{Bi})(1 - e^{(-\mathrm{SSc}/\mathrm{Si})}), \quad (1)$$

where Ai combines the atmospheric path radiance that is attributable to Rayleigh scattering and Mie scattering with the reflectance from clear water, Bi is the increase in exoatmospheric reflectance from Ai to the asymptotic reflectance saturation level at high suspended sediment concentration, and Si is a concentration parameter equal to the suspended sediment concentration when exoatmospheric reflectance is 63% of the difference between average atmospheric path reflectance and the saturation reflectance value. The parameters Ai, Bi, and Si are functions of wavelength. Based on the data presented by Moore (1977), that atmospheric scattering accounts for over 95% of the signal measured by a satellite sensor over clear deep water, the Ai term is comprised primarily of atmospheric path radiance with an almost negligible contribution from reflectance by clear water. The transferability of this exponential model to lakes and reservoirs other than Lake Chicot has been documented (Ritchie et al., 1989; Harrington et al., 1990).

Empirical relationships between suspended sediment concentration and both Secchi depth (Fig. 2) and nephelometric turbidity (Fig. 3) were used to transform Eq. (1). Based on the work of Swain (1980), the form of the relationship between Secchi disk depth (SD) and suspended sediment concentration (SSc) for Lake Chicot is

$$\mathrm{SD} = (D)(\mathrm{SSc})^{-n}, \quad (2)$$

where D is a constant and the exponent n is approximately 2/3. Data from Site 7 at Lake Chicot were used in an optimization routine to determine the value of D and the coefficient of determination. The relationship between Secchi disk depth (cm) and suspended sediment concentration for the waters of Lake Chicot (based on 199 data observations from Site 7) is

$$\mathrm{SD} = (3.978)(\mathrm{SSc})^{-2/3} \quad (3)$$

and the coefficient of determination is $r^2 = 0.701$. Solving for SSc and then substituting the result in Eq. (1) yields

$$\mathrm{Ri} = \mathrm{Ai} + (\mathrm{Bi})(1 - e^{[-(\mathrm{Zi}/\mathrm{SD})^{3/2}]}), \quad (4)$$

where Ri, Ai, and Bi are as defined for Eq. (1) and Zi is a Secchi depth parameter (cm) that can be solved for a specific value of Si using Eq. (3).

Based on the graphical distribution of nephelometric turbidity (T) plotted against suspended sediment concentration (SSc) (Fig. 3), a linear model was used to relate suspended sediment concentration with turbidity. The equation, based on 182 data observations, is

$$T = 4.18 + (0.913)(\mathrm{SSc}) \quad (5)$$

with a coefficient of determination of $r^2 = 0.877$.

Figure 2. Scatterplot of the relationship between Secchi disk depth and suspended sediment concentration (mg L^{-1}) including the equation: $\mathrm{SD} = (3.978)(\mathrm{SSc})^{-2/3}$.

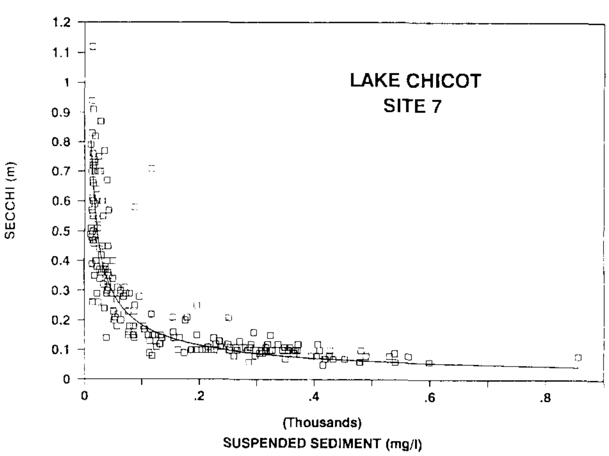

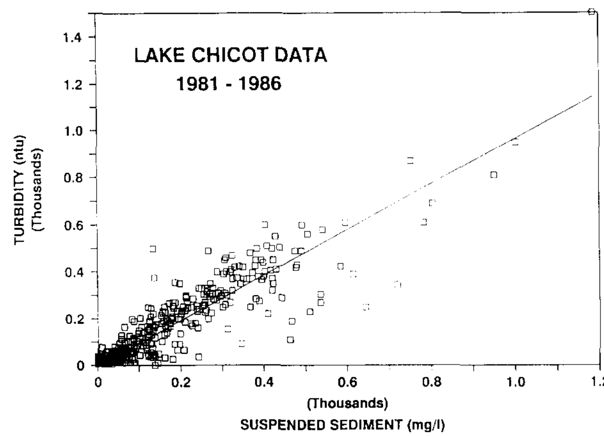

Figure 3. Scatterplot of the relationship between nephelometric turbidity and suspended sediment concentration including the equation: $T = (0.927)(\mathrm{SSc})$.

Equation (5) was simplified to set the Y-intercept to zero (i.e., eliminate the small Y-intercept term). Two things were considered: 1) If the only light scattering particles in the water column are suspended sediments, then the Y-intercept should be zero, and 2) the data value ranges for both nephelometric turbidity and suspended sediment concentration were well over 500 units, thus making the small Y-intercept value negligible. The resulting relationship is

$$T = (0.927)(\mathrm{SSc}), \tag{6}$$

with a coefficient of determination of $r^2 = 0.876$. No significant change in the strength of the statistical relationship occurred with the elimination of the Y-intercept term.

Inserting turbidity T into Eq. (1) was significantly simpler using Eq. (6) rather than Eq. (5) and yielded

$$\mathrm{Ri} = \mathrm{Ai} + (\mathrm{Bi})(1 - e^{(-T/\mathrm{Xi})}), \tag{7}$$

where Xi is a nephelometric turbidity parameter that can be solved for a specific suspended sediment concentration using Eq. (6).

RESULTS AND DISCUSSION

Application of a simple linear regression model to the nontransformed suspended sediment data resulted in relatively low coefficients of determination (r^2 values) for all MSS Bands, with MSS Band 3 performing the best (Table 1). These results are presented for comparison purposes only, since it has been shown that a linear model is inappropriate for this relationship (Munday and Alfoldi, 1979; Curran and Novo, 1988; Harrington et al., 1990).

Improved correlations over a linear model have been demonstrated in previous research using a natural logarithm transformation on the variables (e.g., Carpenter and Carpenter, 1983; Lillesand et al., 1983; Lindell et al., 1986). There is an improvement in model predictability for the visible wavelengths (MSS Bands 1 and 2), but coefficients of determination decline for the infrared wavelengths (MSS Bands 3 and 4) (Table 1).

Suspended Sediment Concentration

The largest coefficients of determination between exoatmospheric reflectance and suspended sediment concentration were obtained (for all four Landsat MSS Bands) with optimized curve-fitting and Eq. (1) (Table 1 and Figs. 4a–d). The best overall relationship, $r^2 = 0.716$, was obtained for Landsat MSS Band 3, the 700–800 nm wavelength band (Fig. 4c). This observation, that the best wavelengths for satellite assessment of suspended sediment concentration are in the near infrared, is in line with previous research conclusions (e.g., Ritchie et al., 1976; 1983; Ritchie and Schiebe, 1986; Schiebe and Ritchie, 1986).

Examination of the model coefficients provides additional support for use of the exponential model [Eq. (1)]. The average atmospheric path radiance (Ai), which is a function of Rayleigh scattering, is greatest for Landsat MSS Band 1 and declines with increasing wavelength. Bi is the magnitude of the exoatmospheric reflectance difference between 1) the combined background noise provided by atmospheric scattering and the

Table 1. Coefficients of Determination (r^2 values), Standard Errors of Estimates (in Parentheses), and Optimized Values of Coefficients (Ai, Bi, and Si) from Analysis of 310 Observations of Suspended Sediment Concentration (SSc) and Exoatmospheric Reflectance (EREF)[a]

EREF (i)[b]	*Linear (SSc)*	*LN (SSc)*	*Exponential*	*Ai*	*Bi*	*Si*
1	0.285 (0.028)	0.367 (0.198)	0.476 (0.024)	0.105	0.071	90.9
2	0.500 (0.036)	0.541 (0.292)	0.700 (0.028)	0.066	0.138	130.3
3	0.618 (0.030)	0.512 (0.317)	0.716 (0.026)	0.057	0.160	266.6
4	0.468 (0.023)	0.254 (0.138)	0.489 (0.026)	0.040	0.130	598.4

[a] Based on the NASA Standard solar spectral irradiance curve, where Linear (SSc) column provides coefficients of determination for simple linear regression on the non-transformed data, the LN (SSc) column is for simple linear regression using a natural logarithm transform on both SSc and EREF, and the Exponential column has r^2 values for the theoretically derived exponential curve.

[b] Wavelength bands correspond with the Landsat MSS numerical designation band used for Landsat's 4 and 5.

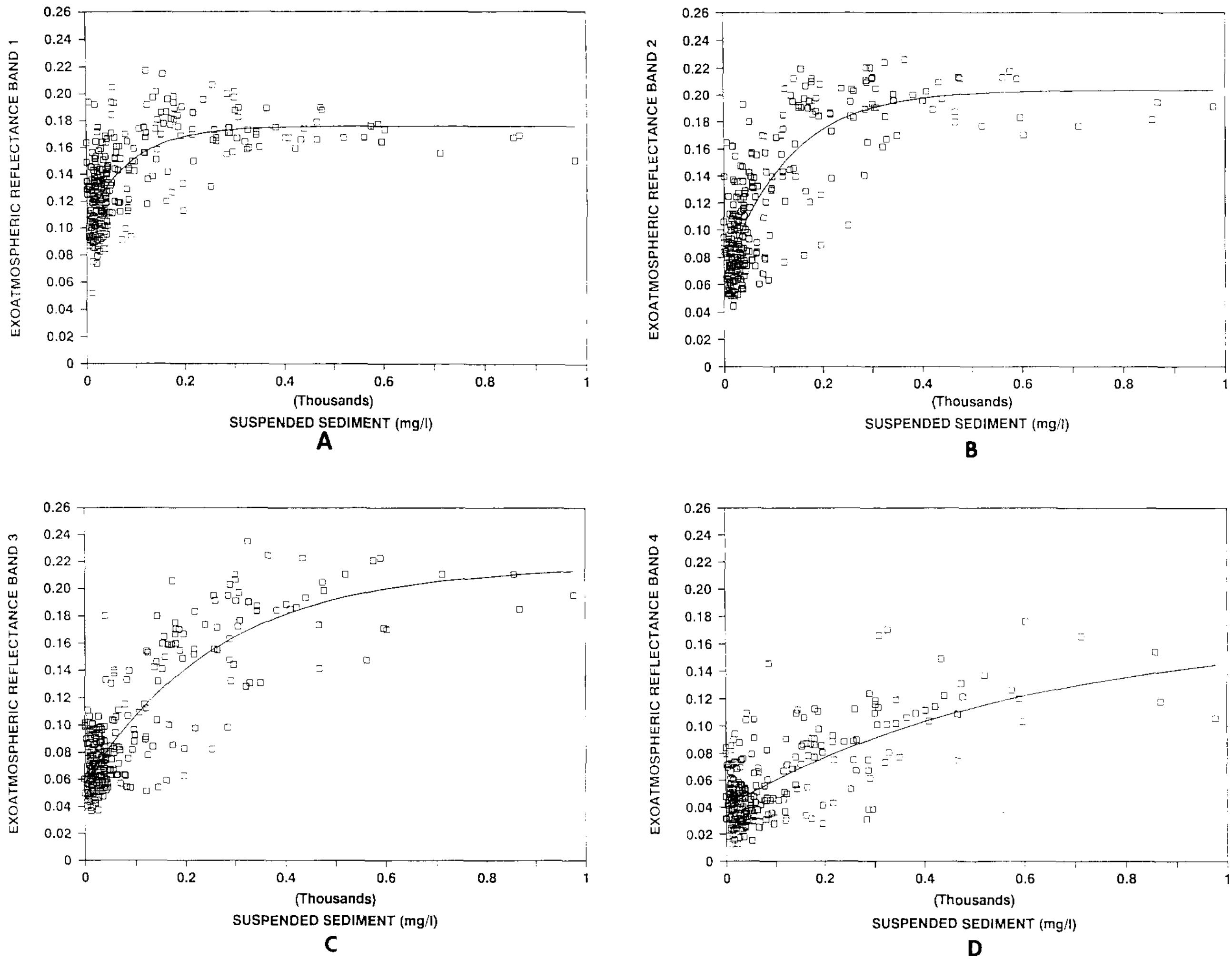

Figures 4a–d. Scatterplots and best-fit curves for the relationships between exoatmospheric reflectance and suspended sediment concentration.

reflectance from clear water (Ai) and 2) saturation at an asymptotic value (Ai + Bi). The Bi coefficient indicates the sensitivity of the model to discriminate differences in suspended sediment concentration with variations in exoatmospheric reflectance. A greater precision can be obtained with estimates of suspended sediment concentration based on the use of Landsat MSS Band 3 as a result of the larger magnitude Bi statistic.

The Si coefficient is indicative of the center of the range of suspended sediment concentrations that can be assessed using a specific wavelength band (i). The increasing value of the Si coefficient with increasing wavelength combined with the magnitude of the Bi coefficient results in the following interpretations: 1) For Landsat MSS Band 1, exoatmospheric reflectance measures are highly sensitive to low suspended sediment concentrations and reflectance quickly saturates with increasing sediment loads (Fig. 4a); 2) Landsat MSS Band 3 provides the greatest ability to monitor the range of suspended sediment levels that are of most concern in lake resource management (i.e., 0–500 mg L^{-1}) (Fig. 4c); and 3) for Landsat MSS Band 4, exoatmospheric reflectance is most sensitive to very high suspended sediment loads (Fig. 4d).

This exponential model has been tested using data from other lakes and reservoirs (Ritchie et al., 1989; Menzel et al., 1989; Harrington et al., 1990) and used in a predictive way to assess water quality conditions for lakes where no ground truth data were available (Harrington et al., forthcoming). Care must be exercised in using this exponential model for assessment of minor variations among clear lakes because the atmospheric path

Table 2. Same as Table 1 Except for the Use of the Variable Secchi Disk Depth (SD) in Place of SSc–272 Observations

EREF (i)	*Linear (SD)*	*LN (SD)*	*Exponential*	*Ai*	*Bi*	*Zi*
1	0.340 (0.026)	0.383 (0.194)	0.467 (0.024)	0.105	0.071	19.4
2	0.519 (0.035)	0.601 (0.267)	0.715 (0.026)	0.066	0.138	15.2
3	0.444 (0.035)	0.605 (0.279)	0.694 (0.026)	0.057	0.160	9.4
4	0.226 (0.028)	0.321 (0.423)	0.424 (0.023)	0.040	0.130	5.5

radiance and clear water reflectance term, Ai, incorporates substantial variability in atmospheric conditions over time or space. Thus, the Ai term in the model is a source of uncertainty for satellite-derived estimates of surface condition. This uncertainty is especially troublesome at low concentrations of suspended sediments because the signal to noise ratio becomes quite small.

Secchi Disk Depth

Application of a linear model for the relationship between exoatmospheric reflectance and Secchi disk depth results in relatively low coefficients of determination (Table 2), with the best relationship obtained for Landsat MSS Band 2. Use of a natural logarithm transform on both variables and simple linear regression analyses results in improved coefficients of determination and approximately equal performance by Landsat MSS Bands 2 and 3 (Table 2).

Coefficients of determination from either set of simple linear regression analyses are lower in comparison with the r^2 values obtained from the application of the modified exponential model (Eq. 4) to the 272 observations of exoatmospheric

Figures 5a–d. Scatterplots and best-fit curves for the relationships between exoatmospheric reflectance and Secchi disk depth.

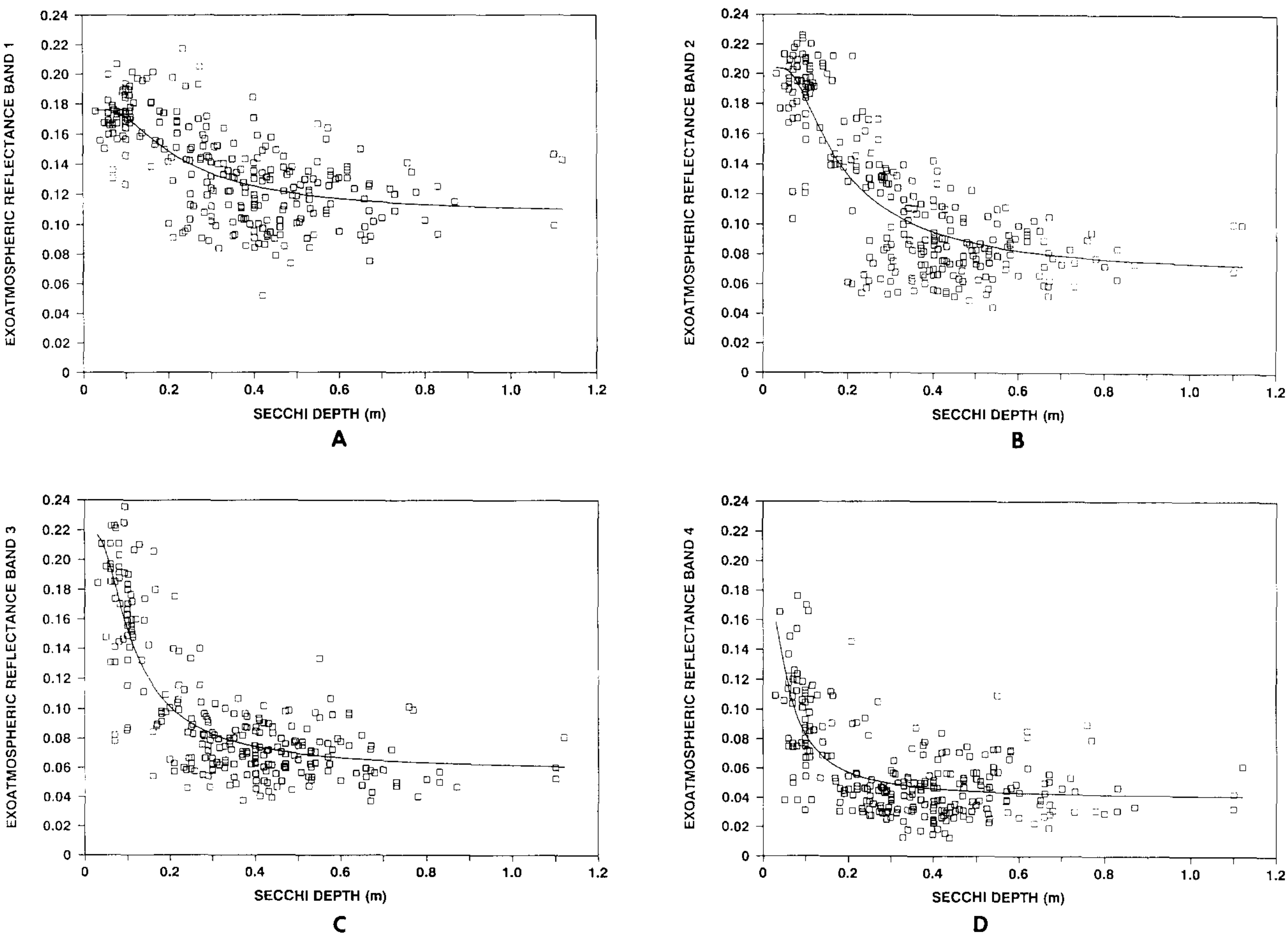

Table 3. Same as Table 1 Except for the Use of the Variable Nephelometric Turbidity (*T*) in Place of SSc – 187 Observations

EREF (i)	*Linear (T)*	*LN (T)*	*Exponential*	*Ai*	*Bi*	*Xi*
1	0.448 (0.023)	0.524 (0.169)	0.619 (0.020)	0.105	0.071	84.3
2	0.634 (0.032)	0.711 (0.239)	0.821 (0.021)	0.066	0.138	120.8
3	0.712 (0.025)	0.682 (0.250)	0.812 (0.019)	0.057	0.160	247.2
4	0.618 (0.016)	0.465 (0.304)	0.638 (0.015)	0.040	0.130	554.9

reflectance, and Secchi disk depth (Table 2 and Figs. 5a–d). Landsat MSS Band 2, the visible red wavelengths from 600–700 nm, provides the highest r^2 value (Table 2 and Fig. 5b). Values of the Ai and Bi coefficients were held constant (at the values that were determined for the suspended sediment concentration models – Table 1) in these optimization runs. Results suggest that Landsat MSS Bands 2 and 3 are similar and have the greatest capability for discriminating variations in Secchi disk depth based on variations in exoatmospheric reflectance. The Zi coefficient indicates the center of the range of Secchi disk depths (cm) for which an individual wavelength band (i) will perform the best. Larger Zi values for the shorter wavelengths imply that shorter wavelengths should be used to monitor water columns with fewer contaminants.

Nephelometric Turbidity

The largest coefficients of determination between exoatmospheric reflectance and any of the measures of surface water quality are with nephelometric turbidity (Table 3). Simple linear regression analyses involving the use of the raw data suggests that Landsat MSS Band 3 provides the best predictive ability given a linear model. Little, if any, improvement is obtained by the use of a natural logarithm transformation prior to simple linear regression analysis (Table 3).

Application of the exponential model [Eq. (7)] to the Lake Chicot data set of 187 corresponding observations of nephelometric turbidity and exoatmospheric reflectance resulted in the largest coefficients of determination of any of the models tested (Table 3 and Figs. 6a–d). A value of $r^2 = 0.821$ for Landsat MSS Band 2 is the highest overall (Fig. 6b) and the value of $r^2 = 0.812$ for Landsat MSS Band 3 is also good (Fig. 6c). As before, the atmospheric path radiance term Ai and the Bi coefficient were held constant in model optimization.

The Xi coefficient provides information similar to that provided by the Si coefficient used in the suspended sediment relationship (i.e., that longer wavelengths provide better analytical capabilities for more turbid water bodies) (Table 3). These results indicate that the red (600–700 nm) and near infrared (700–800 nm) wavelengths provide the greatest ability for estimating nephelometric turbidity variations using Landsat MSS data.

Comparison of Results Using Different Solar Spectral Irradiance Curves

Equations (1), (4), and (7) were used to examine the effects of substituting the solar spectral irradiance curve proposed by the World Radiation Center (Iqbal, 1983) for the NASA standard curve (Thekaekara, 1970) and the relative contribution of including an eccentricity correction factor in the calculation of exoatmospheric reflectance (EREF). Table 4 provides the coefficients of determination derived from empirical model optimization for three different scenarios: 1) the NASA standard curve, 2) the NASA standard curve with the inclusion of an eccentricity correction factor, and 3) the EREF calculated using the World Radiation Center proposed solar curve and modified by the eccentricity correction factor. Comparison of scenarios 1 and 2 suggests that the addition of an eccentricity correction factor provides little, if any, significant changes. The most pronounced changes (decreases) are for Landsat MSS Band 4 (800–1100 nm). It has been hypothesized prior to including the eccentricity correction factor that slight improvements in predictive capability (higher r^2 values) would result. Comparison of scenarios 2 and 3 indicates that use of the NASA spectrum in calculating EREF, rather than the

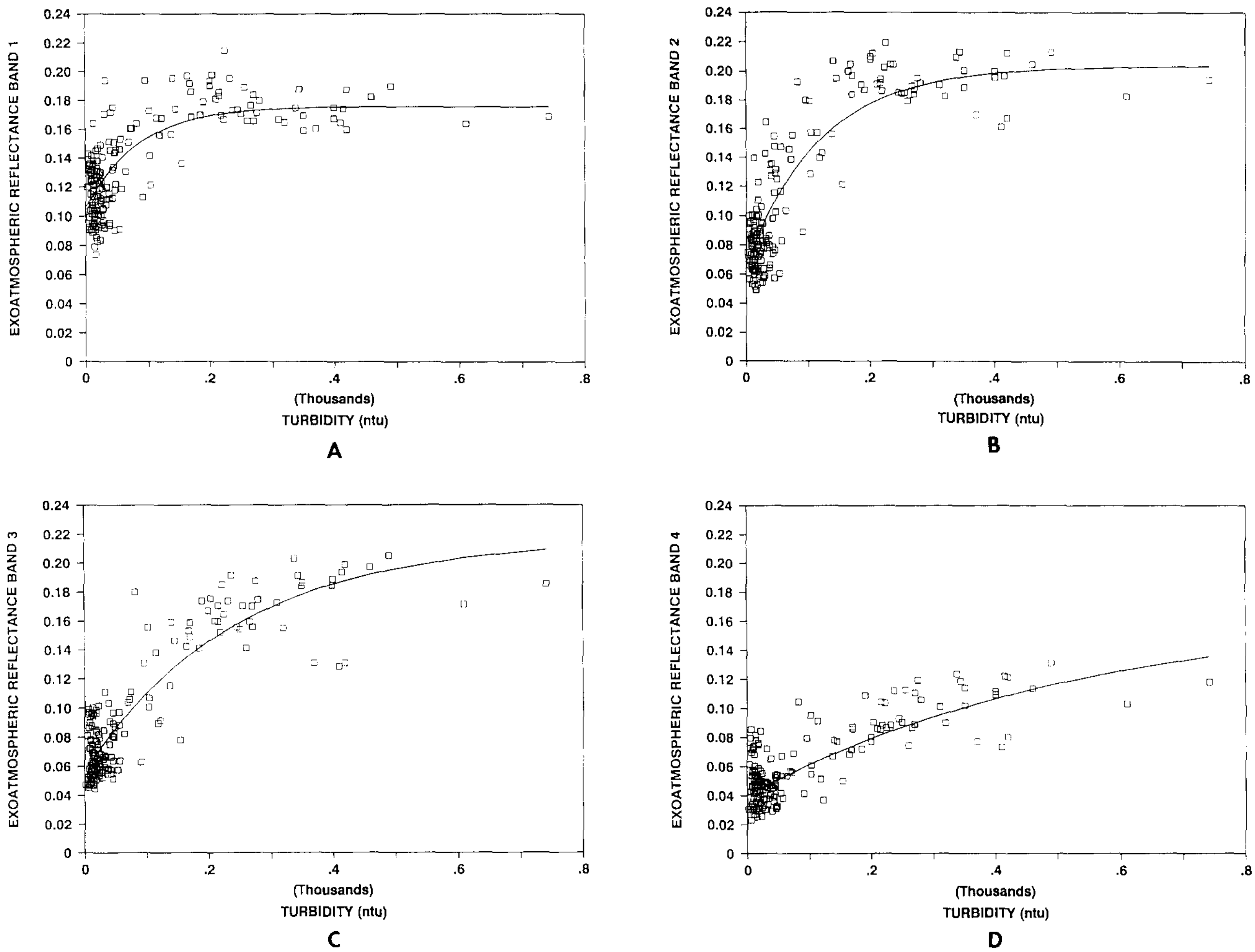

Figures 6a–d. Scatterplots and best-fit curves for the relationships between exoatmospheric reflectance and nephelometric turbidity.

Table 4. Coefficients of Determination for Optimized Exponential Relationships between Water Quality Measures and Exoatmospheric Reflectance (EREF)[a]

Water Quality Variable	*EREF (i)*	*NASA*	*NASA + Ecc*	*WRC + Ecc*
SSc	1	0.476	0.472	0.476
	2	0.700	0.697	0.684
	3	0.716	0.707	0.670
	4	0.489	0.471	0.422
SD	1	0.467	0.469	0.467
	2	0.715	0.716	0.726
	3	0.694	0.683	0.689
	4	0.424	0.405	0.406
T	1	0.619	0.612	0.555
	2	0.821	0.817	0.790
	3	0.812	0.796	0.742
	4	0.638	0.624	0.548

[a] The NASA column indicates use of the NASA standard solar spectral irradiance curve in calculating exoatmospheric reflectance, the NASA + Ecc column indicates EREF calculations using the NASA curve and an eccentricity correction factor, and the WRC + Ecc column indicates EREF calculations using the solar curve proposed by the World Radiation Center and using an eccentricity correction factor.

spectum recommended by the World Radiation Center, improves the coefficients of determination, especially in the longer wavelengths. Since there are good arguments for the World Radiation Center's solar spectral irradiance curve, these results suggest that conclusions of previous investigations based on the use of the NASA standard curve may be slightly optimistic for the near infrared wavelengths.

Digital Chromaticity Indices

Results from the application of a linear model to the relationships between the chromaticity indices and the natural logarithm transform of the water quality measures indicate that the x chromaticity index provides greater predictive capability (Table 5 and Figs. 7a–c). As was the case with the other analyses, models involving the use of optical measures of water quality (i.e.,

Table 5. Coefficients of Determination for Simple Linear Regression Analyses between Chromaticity Indices and Natural Logarithm Transformations of Measures of Water Quality

Chromaticity Index	*LN (SSc)*	*LN (SD)*	*LN (T)*
x	0.474	0.543	0.735
y	0.351	0.335	0.604
z	0.194	0.251	0.344

nephelometric turbidity and Secchi disk depth) had better correlations (Table 5) and nephelometric turbidity provided the best correlation. In all cases, the use of the theoretically derived exponential model [Eqs. (1), (4), and (7)] resulted in better coefficients of determination than the use of chromaticity indices.

SUMMARY AND CONCLUSION

Based on 12 years of Landsat MSS data observations of Lake Chicot, Arkansas, involving 79 different dates, the ability to assess variations in surface water quality characteristics from a space-based platform is clearly demonstrated. Although uncertainty exists within the satellite-based assessments due to the variable contribution of atmospheric path radiance, we believe the method presented herein is an acceptable alternative to the costs associated with making numerous in situ samples. In general, the Landsat MSS Bands that cover the visible red (600–700 nm) and near infrared (700–800 nm) wavelengths are considered more appropriate than other wavelength bands for predicting surface water quality characteristics. Of the three water quality variables that were analyzed in this research, the optical measures (i.e., nephelometric turbidity and Secchi disk depth) were associated with larger coefficients of determination and nephelometric turbidity was consistently the highest. In all cases analyzed, the theoretically derived exponential model provided a better fit with the data.

Technical assistance by F. E. Morrison throughout the 9 years that it has taken to assemble and analyze this data set is gratefully acknowledged. Interagency cooperation and funding for the water quality data collection and laboratory analyses was provided by the U. S. Army Corps of Engineers, Vicksburg District. Data collection during the course of the project has been performed by personnel from Quachita Baptist Univer-

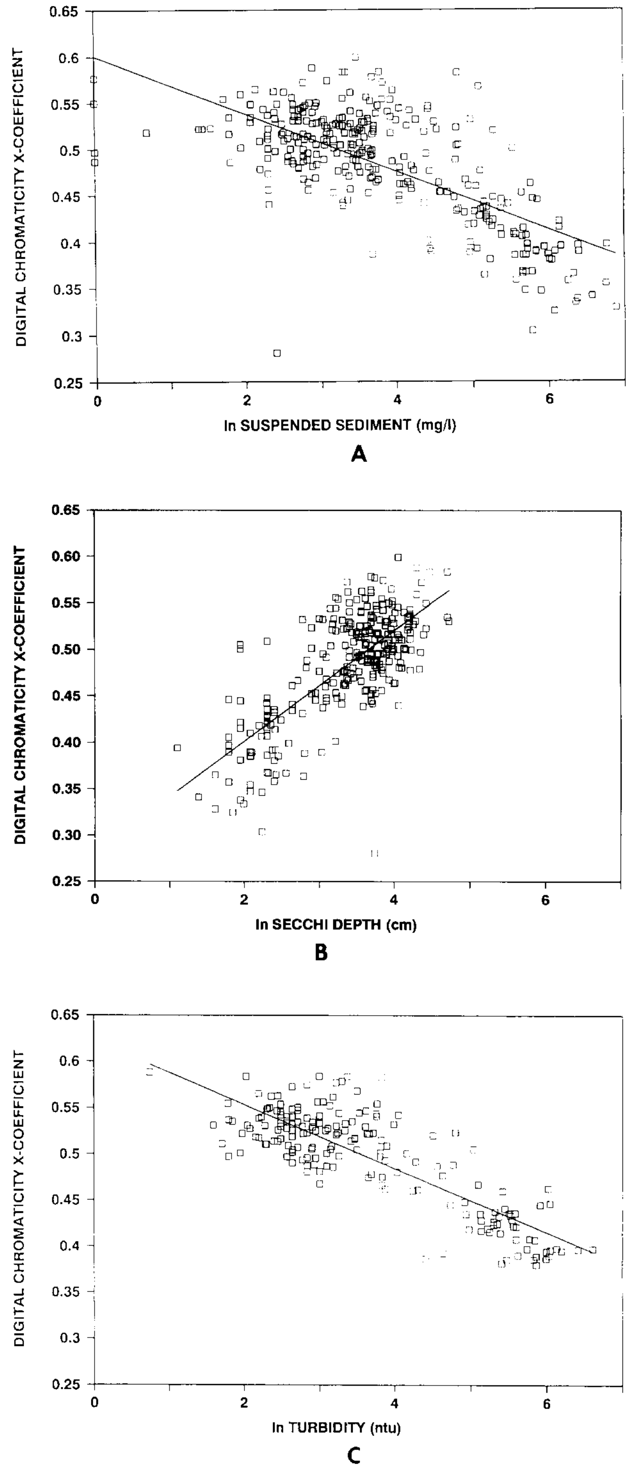

Figures 7a–c. Scatterplots and best-fit curves for the relationships between the *x* digital chromaticity index and suspended sediment concentration, Secchi disk depth, and nephelometric turbidity.

sity, the Agricultural Research Service, and the U. S. Army corps of Engineers. Manuscript reviews by Drs. Susan Berta and M. Duane Nellis are greatly appreciated.

REFERENCES

Carlson, R. E. (1977), A trophic state index for lakes, *Limnol. Oceanogr.* 22:361–369.

Carpenter, D. S., and Carpenter, S. M. (1983), Monitoring inland water quality using Landsat data, *Remote Sens. Environ.* 13:345–352.

Curran, P. J., and Novo, E. M. M. (1988), The relationship between suspended sediment concentration and remotely sensed spectral radiance: a review, *J. Coastal Res.* 4:351–368.

DeCoursey, D. G., and Snyder, W. M. (1969), Computer-oriented method of optimizing hydrologic model parameters, *J. Hydrol.* 9:34–56.

Harrington, J. A., Jr., Schiebe, F. R., and Morrison, F. E. (1989), Monitoring lake quality with the Landsat MSS, in *Regional Characterization of Water Quality* (S. Ragone, Ed.), IAHS, Baltimore, MD, Publ. No. 182, pp. 143–150.

Harrington, J. A., Jr., Schiebe, F. R., and Ross, J. D. (1990), A method for mapping the spatial distribution of suspended sediments within lakes or reservoirs using Landsat Multispectral Scanner data, in *Proceedings, Remote Sensing and GIS Applications to Nonpoint Source Planning,* 1–3 October 1990, US EPA, Chicago, IL, pp. 103–111.

Harrington, J. A., Jr., Schiebe, F. R., Ross, J. D., Morrison, F. E., and Cauthron, W. L. (forthcoming), Oklahoma Lake Assessment Using Multidate Landsat MSS Data.

Iqbal, M. (1983), *An Introduction to Solar Radiation*, Academic, New York.

Lathrop, R. G., Jr., and Lillesand, T. M. (1986), Use of Thematic Mapper data to assess water quality in Green Bay and central Lake Michigan, *Photogramm. Eng. Remote Sens.* 52:671–680.

LeCroy, S. R. (1982), Determination of turbidity patterns in Lake Chicot from LANDSAT MSS imagery, NASA Contractor Report 165870, Langley Research Center, Hampton, VA.

Lillesand, T. M., Johnson, W. L., Deuell, R. L., Lindstrom, O. M., and Meisner, D. E. (1983), Use of Landsat data to predict the trophic state of Minnesota lakes, *Photogramm. Eng. Remote Sens.* 49:219–229.

Lindell, T., Karlsson, B., Rosengren, M., and Alfoldi, T. (1986), A further development of the chromaticity technique for satellite mapping of suspended sediment load, *Photogramm. Eng. Remote Sens.* 52:1521–1529.

Lyon, J. C., Bedford, K. W., Yen, J. C., Lee, D. H., and Mark, D. J. (1988), Determinations of suspended sediment from multiple day Landsat and AVHRR data, *Remote Sens. Environ.* 25:107–115.

Markham, B. L., and Barker, J. L. (1986), Landsat MSS and TM post-calibration dynamic ranges, exoatmospheric reflectances and at-satellite temperatures, *EOSAT Tech. Notes* 1:3–8.

Menzel, R. G., Troeger, W. W., and Schiebe, F. R. (1989), Properties of selected Oklahoma lakes in relation to remote sensing of suspended sediment, *Lake Reservoir Manage.* 5(2):31–37.

Moore, G. K. (1977), Satellite surveillance of physical water-quality characteristics, in *Proceedings of the 12th International Symposium on Remote Sensing of Environment,* University of Michigan, Ann Arbor, pp. 445–461.

Munday, J. C., Jr., and Alfoldi, T. T. (1979), Landsat test of diffuse reflectance models for aquatic suspended solids measurement, *Remote Sens. Environ.* 8:169–183.

Nix, J. F., and Schiebe, F. R. (1984), *Limnological Studies of Lake Chicot, Arkansas*: Ouachita Baptist University Press, Arkadelphia, AR.

Ritchie, J. C., and Cooper, C. M. (1987), Comparison of Landsat MSS pixel array sizes for estimating water quality, *Photogramm. Eng. Remote Sens.* 53:1549–1553.

Ritchie, J. C., and Cooper, C. M. (1988), Comparison of measured suspended sediment concentrations with suspended sediment concentrations estimated from Landsat MSS data, *Int. J. Remote Sens.* 9:379–387.

Ritchie, J. C., and Schiebe, F. R. (1986), Monitoring suspended sediments with remote sensing techniques, in *Hydrologic Applications of Space Technology,* IAHS Publ. No. 160; pp. 233–243.

Ritchie, J. C.., Schiebe, F. R., and McHenry, J. R. (1976), Remote sensing of suspended sediments in surface waters, *Photogramm. Eng. Remote Sens.* 42:1539–1545.

Ritchie, J. C., Schiebe, F. R., and Cooper, C. M. (1983), Spectral measurements of surface suspended matter in an oxbow lake in the lower Mississippi Valley, *J. Freshwater Ecol.* 2:175–181.

Ritchie, J. C., Schiebe, F. R., and Cooper, C. M. (1986), Surface water quality measurements of Lake Chicot, Arkansas using data from Landsat satellites, *J. Freshwater Ecol.* 3:391–397.

Ritchie, J. C., Cooper, C. M., and Yongqing, J. (1987), Using Landsat multispectral scanner data to estimate suspended sediments in Moon Lake, Mississippi: *Remote Sens. Environ.* 23:65–81.

Ritchie, J. C., Schiebe, F. R., and Cooper, C. M. (1989), Landsat digital data for estimating suspended sediment in inland water: in *Regional Characterization of Water Quality* (S. Ragone, Ed.), IAHS Publ. No. 182, pp. 151–158.

Robinove, C. J. (1982), Computation of physical values for Landsat digital data, *Photogramm. Eng. Remote Sens.* 48: 781–784.

Schiebe, F. R., and Ritchie, J. C. (1986), Suspended sediment monitored by satellite, in *Proceedings, Fourth Federal*

Interagency Sedimentation Conference, Las Vegas, NV, Vol. 1, pp. 70–78.

Schiebe, F. R., Ritchie, J. C., and Boatwright, G. O. (1985), A first evaluation of Landsat TM to monitor suspended sediment in lakes, in *Landsat-4 Science Characterization Early Results*, NASA Conference Publication 2355, Vol. 4, pp. 337–347.

Schiebe, F. R., Harrington, J. A., Jr., and Ritchie, J. C. (1987), Remote sensing of suspended sediments of Lake Chicot, Arkansas, in *U. S. Army Corps of Engineers, Sixth Remote Sensing Symposium Proceedings*, Galveston, TX, 2–4 November, pp. 7–85.

Schiebe, F. R., Harrington, J. A., Jr., and Ritchie, J. C. (forthcoming), Remote Sensing of Suspended Sediments, The Lake Chicot, Arkansas Project, *Int. J. Remote Sens.* (in press).

Shih, S. F., and Gervin, J. C. (1980), Ridge regression techniques applied to Landsat investigation of water quality in Lake Okeechobee, *Water Resources Bull.* 16:790–796.

Stefan, H.G., Dhamotharan, S., Fu, A. Y., and Cardoni, J. J. (1984), Mathematical model simulation of Lake Chicot, Arkansas, in *Limnological Studies of Lake Chicot, Arkansas* (J. F. Nix and F. R. Schiebe, Eds.), Ouachita Baptist University, Arkadelphia, AR.

Swain, A. (1980), Material budgets of Lake Chicot, Ph.D. dissertation, University of Mississippi, Oxford, 190 pp.

Thekaekara, M. P. (1970), *The solar constant and the solar spectrum measured from a research aircraft*, NASA Tech. Report R-351, Goddard Space Flight Center, Greenbelt, MD 20771.

USGS (1979), *National Handbook of Recommended Methods for Water Data Acquisition*, Office of Water Data Coordination, USGS, Reston, VA.

Verdin, J. P. (1983), Corrected vs. uncorrected Landsat-4 MSS data, *Landsat Data Users Notes* 27:4–8.

Verdin, J. P. (1985), Monitoring water quality in a large western reservoir with Landsat imagery, *Photogramm. Eng. Remote Sens.* 51:343–353.

Welch, R. A., Jordan, T. R., and Usery, E. L. (1983), Microcomputers in the mapping sciences, *Comput. Graphics World* 6(2):6–10.

Witte, W. G., Whitlock, C. H., Usry, J. W., Morris, W. D., and Gurganus, E. A. (1981), *Laboratory measurements of physical, chemical and optical characteristics of Lake Chicot sediment waters*, NASA Tech. Paper 1941, Langley Research Center, Hampton, VA.